33RD INTERNATIONAL COSMIC RAY CONFERENCE, RIO DE JANEIRO 2013
THE ASTROPARTICLE PHYSICS CONFERENCE

ICRC 2013

Study of neutral baryon production at the very forward region of the LHC

K. KAWADE[1], O. ADRIANI[2,3], L. BONECHI[2], M. BONGI[3], G. CASTELLINI[4], R. D'ALESSANDRO[2,3], M. HAGENAUER[5], Y. ITOW[1,6], K. KASAHARA[7], Y. MAKINO[1], K. MASUDA[1], E. MATSUBAYASHI[1], H. MENJO[8], G. MITSUKA[1], Y. MURAKI[1], P. PAPINI[2], A-L. PERROT[9], D. PFEIFFER[9], S. RICCIARINI[2,4], T. SAKO[1,6], Y. SHIMIZU[10], T. SUZUKI[7], T.TAMURA[11], S. TORII[7], A. TRICOMI[12,13], AND W.C. TURNER[14]

[1] *Solar-Terrestrial Environment Laboratory, Nagoya University, Japan*
[2] *INFN Section of Florence, Italy*
[3] *University of Florence, Italy*
[4] *IFAC-CNR, Italy*
[5] *Ecole-Polytechnique, France*
[6] *Kobayashi-Maskawa Institute for the Origin of Particles and the Universe, Nagoya University, Japan*
[7] *RISE, Waseda University, Japan*
[8] *Graduate school of Science, Nagoya University, Japan*
[9] *CERN, Switzerland*
[10] *JAXA, Japan*
[11] *Kanagawa University, Japan*
[12] *INFN Section of Catania, Italy*
[13] *University of Catania, Italy*
[14] *LBNL, Berkeley, USA*

kawade@stelab.nagoya-u.ac.jp

Abstract:
The LHCf experiment is dedicated to verify the hadronic interaction models used in cosmic-ray physics. Forward baryon production is one of the keys to understand the air shower development. A preliminary results of neutral baryon spectra measured at very forward region of LHC $\sqrt{s}$ = 7TeV p-p collisions are presented in this paper. The responce of the detector for baryon measurement is studied based on MC simulations and a beam test at SPS. Experimental results at LHC are compared with the predictions from the known hadronic interaction models.

Keywords: UHECR, LHC, forward neutron

1 Introduction

Forward particle production in high-energy particle collision is one of the unknown phenomenon and important process in development of cosmic-ray showers. Most of the particles emitted at the forward region are generated from the result of low-x QCD process. Because the coupling constant of the strong interaction diverges in the collision with very low momentum transfer (q^2), the production of forward particles can not be calculated by the perturbation QCD theory. Therefore, phenomenological models based on the Gribov-Regge theory [1, 2] that describes soft process are very important to describe the particle production at very forward rapidity. They should be calibrated by the high-energy collider experiments.

The LHCf experiment [3, 4] is dedicated to verify the hadronic interaction models that describe the forward particle production processes. LHCf measures the particles emitted in the very forward region of LHC (pseudo rapidity $|\eta| > 8.4$). LHCf already published the results from measurements of single photon spectra at $\sqrt{s}$ = 7TeV [5] and at 900GeV [6], and π^0 spectra at 7TeV [7]. In this paper, analysis of the LHCf data for the forward baryon spectra is discussed. If forward baryons have more energy after the collisions, cosmic ray showers can penetrate deeply in the atmosphere, or if less energy, the showers can develop rapidly. So the baryon spectra are very important to understand the behaviour of cosmic-ray showers. The fraction of energy used to generate secondary particles is termed inelasticity k. k can be directly measured by neutral baryon measurement at very forward that provides $1-k$, or elasticity.

The model predictions of neutral baryon (predominantly neutrons) production have quite large difference among the models. Figure.1 shows the energy spectra of neutral baryons predicted by the models, EPOS [8], QGSJET2 [9], SYBILL [10], DPMJET3 [11], and PYTHIA [12]. Detector resolution and trigger efficiency are not considered in this plot. Vertical axis are normalized to event par inelastic collision(Not yet).

2 The performance of LHCF detector for neutron measurement

2.1 The LHCf detector

Two independent detectors named Arm1 and Arm2 are installed in the detector installation slots of the TANs located 140m away from the IP1. Both Arm1 and Arm2 have two different calorimeter towers, called small tower and large tower. Each calorimeter is composed of sampling calorimeters and position sensitive detectors. Each sampling calorimeter consists of 16 layers of scintillator and tungsten plates. Total depth is 44 radiation lengths and 1.6 hadron interaction lengths. Four pairs of X-Y position sensors are inserted between the sampling layers. SciFi detectors are used for Arm1 and silicon strip sensors are used

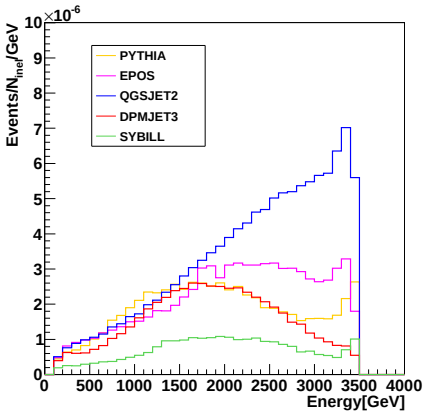

Figure 1: The MC prediction of neutral baryon energy spectra. The colors correspond to each model (see legend).

for Arm2. Because the detector performance for photons was reported elsewhere[13], performance for the neutron measurement is reported in this paper.

2.2 Detector performance

The performance of the LHCf detector for neutrons is studied based on the MC simulations. COSMOS (v7.49) and EPICS (v8.81)[14] those are the MC simulation libraries used in the cosmic-ray simulation are used in this study. Basic calibrations, such as PMT gain, were carried out in a previous study for photon analysis. Here, neutron specified performances are studied.

An offline event selection that is tighter than experimental trigger condition is applied. The selection condition is a coincidence of successive three scintillation layers exceeding a certain threshold. The detection efficiencies of neutrons as a function of incident energy are summarized in figure.2. Flat efficiency up to 70% is achieved above

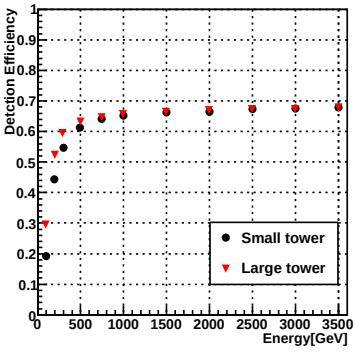

Figure 2: Detection efficiencies of neutrons as a function of energy. Black (Red) markers correspond to the efficiency of the small (large) tower.

500GeV after the offline trigger.

Figure.3 shows the resolution of lateral incident position measured by the position sensitive detector. Depending on incident energy, position resolution from a few mm to 0.5mm is achieved with the same analysis method used in the photon measurement.

Incident energy is estimated from a total energy de-

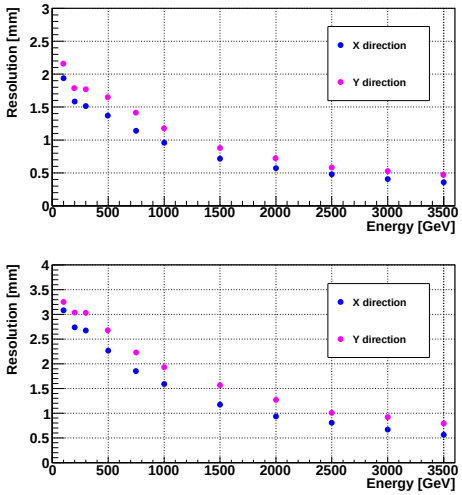

Figure 3: Position resolution for neutrons as a function of energy. Upper and lower panel correspond to the resolution of small tower and large tower, respectively.

posited in the calorimeter. An energy estimator sumdE is defined as,

$$\text{sumdE} = \sum_{2}^{15} n_{step} \times dE_i,$$

where n_{step} are 1 for the 2nd to 10'th layers, and 2 for the 11'th to the last layers (proportional to the tungsten thickness).

Energy response function is determined from the relation between the incident energy "E" and sumdE for each tower as shown in the upper panel of figure.4. The hori-

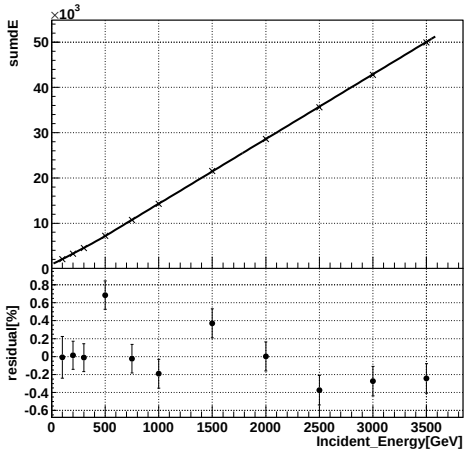

Figure 4: Energy response function. Upper panel shows the relation between the incident energy and means of sumdE. Black curve is a fitting result. Bottom panel shows residual from fitting.

zontal axis corresponds to the energy of the incident neutrons and the vertical axis corresponds to the mean values of sumdE. The response functions are derived by fitting with empirical functions. For the small tower, a function below is used.

$$\text{sumdE} = f(E) = \begin{cases} aE^2 + bE + c & (\text{E} < 500\text{GeV}) \\ dE + e & (500\text{GeV} < \text{E}) \end{cases} \quad (1)$$

Parameters in the function 1 are constraint to smoothly connect at 500GeV. On the other hand, only a quadratic function is used for the large tower. As shown in the bottom panel of figure.4, that is residual from fitting, less than 1% of energy scale non linearity for small tower, and 2% for large tower are confirmed. The error bars indicate the statistical uncertainty.

Figure.5 shows a typical reconstructed energy distribution in case of neutrons with the energy of 1TeV injected at the center of small tower. Black line corresponds to neu-

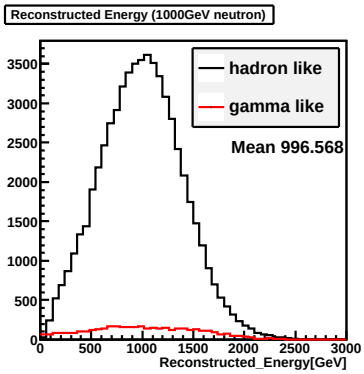

Figure 5: Reconstructed energy of 1TeV neutron.

tron like events, and red line corresponds to gamma like events. Due to the lack of longitudinal depth of the detector for hadronic showers, large fluctuation in the energy estimation is unavoidable. Energy resolution is defined as the standard deviation of the reconstructed energy distribution. Figure.6 shows the energy resolutions of small tower and large tower as functions of incident energy. The MC calcu-

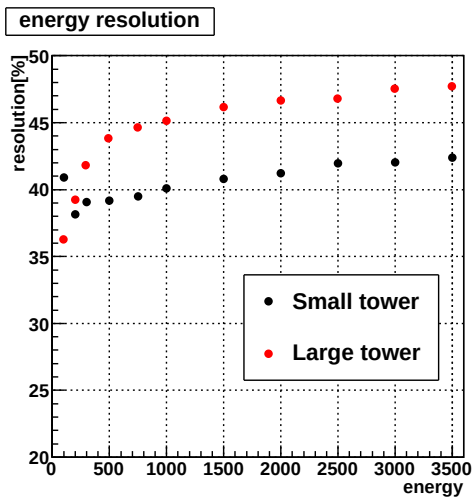

Figure 6: Energy resolutions of small tower (black) and large tower (red) for neutrons as functions of energy.

lation predicts the energy resolution is about 40% for the small tower and 45% for the large tower.

2.3 The SPS beam test

The consistency of the MC simulation was carefully checked by comparing results of the beam tests performed at the CERN-SPS in 2007. In the SPS beam test, the LHCf detectors were exposed to 150GeV and 350GeV proton beams. Trigger signals were generated by the trigger scintillators placed behind the thin beam exit window. Then, precise transverse hit positions were measured by the ADAMO tracker [15] installed in front of the LHCf detector. The ADAMO tracker is composed of the silicon strip sensors with fine position resolution of less than 20 μm.

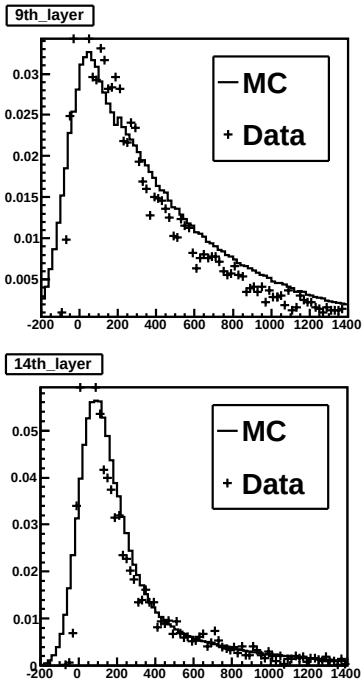

Figure 7: Deposited energy distribution of the 9'th layer (upper) and the 14'th (bottom) layer at the SPS beam test.

Figure.7 shows the deposited energy distribution of the 9'th and the 14'th layer of the calorimeter when 350 GeV proton beams were injected. MC prediction is overlaid by a black line. The 9'th layer have the most large difference among the layers. On the other hand, the 14'th layer shows good agreement between the experimental data and the MC prediction. The difference between the beam test data and the MC prediction will be considered to be a part of systematic uncertainties.

3 The analysis

3.1 Analysis outline

The experimental data for this study was obtained at LHC in May 2010 during $\sqrt{s}$= 7TeV proton-proton collisions. The integrated luminosities were 0.68nb^{-1} for Arm1 and 0.53nb^{-1} for Arm2 after the data acquisition live time was taken into account. The MC data were also generated for about 10^7 inelastic collisions in each model. Same reconstruction methods are used for the experimental data and the MC to avoid analysis bias. Only results from the analysis of the Arm1 detector is presented in this paper.

3.2 Event selection and correction

Because it is difficult to reconstruct the events hitting at the edge of calorimeter, events hitting within 2mm from the edge were removed from the analysis.

Although a lateral shower leakage caused by the limited lateral size of the LHCf detectors smears the energy resolution, using the lateral hit position measured by the position sensors, position depending leakage effects can be corrected.

No efficiency correction was applied because the same reconstruction and analysis processes were applied for both the experimental data and MC simulations.

3.3 PID

Particle Identification (PID) is an important process in the data analysis. A two dimensional PID with $L_{20\%}$ and $L_{90\%}$ parameters is employed to perform PID efficiently with less contamination between neutrons and photons. Here the $L_{20\%}$ and $L_{90\%}$ parameters are the depths containing 20% and 90% of the total deposited energy, respectively. Electromagnetic showers can develop shallowly compared with hadronic showers. PID criteria are chosen to maximize efficiency times purity based on the MC simulation.

Because the ratio of neutron signal to photon contamination depends on the interaction model, the template fitting method based on [16] is introduced to estimate the PID purity correctly. Two different fitting methods are performed, and the difference between them is taken into account as a part of systematic uncertainties.

3.4 Results

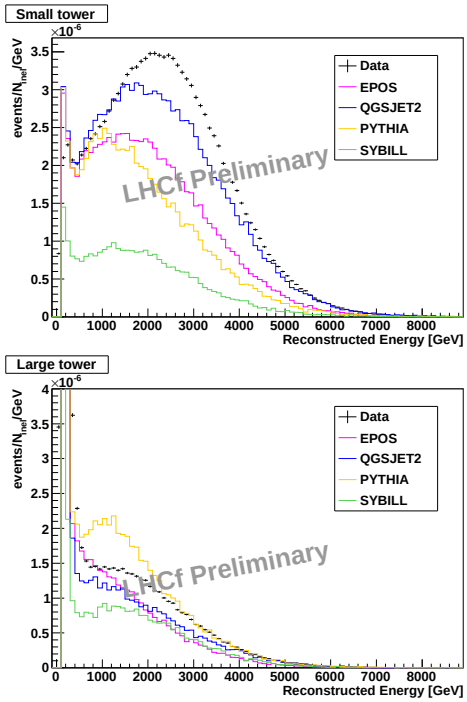

Figure 8: Measured energy spectra of neutron-like events together with the MC predictions. Upper and bottom panels are the results for the small tower and the large tower, respectively. The vertical bars represent the statistical uncertainties. Systematic uncertainty is not included.

Figure.8 shows the energy spectra of forward neutrons measured by the Arm1 detector together with the MC predictions. Black points indicate the measured neutron spectra at $\sqrt{s}$ = 7TeV p-p collisions. Colored lines indicate MC predictions by EPOS 1.99 (magenta), QGSJET II-03 (blue), SIBYLL 2.1 (green), and PYTHIA 8.145 (yellow). As for MC simulations, 5.0×10^6 to 1.0×10^7 inelastic collisions were generated with a detector simulation using the EPICS and COSMOS libraries. Upper and bottom panels correspond to the spectra of the small tower and the large tower, respectively. Vertical axis is normalized to events per number of inelastic collision per GeV. No model matches with the data perfectly.

4 Conclusions

The LHCf successfully completed the phase 1 operation at $\sqrt{s}$ = 7TeV and 900GeV p-p collisions. In this paper, the first analysis of the neutral baryon spectra at the very forward region of LHC $\sqrt{s}$=7TeV p-p collisions are presented. Comparing with the MC predictions, no model can reproduce the results of LHCf perfectly. Studies about systematic errors are still ongoing.

References

[1] V. Gribov, Sov. Phys. JETP **26**, 414 (1968).
[2] T. Regge, Nuovo Ciment, **14**, 951-976 (1959).
[3] O. Adriani et al., LHCf-TDR, CERN-LHCC-2006-004
[4] O. Adriani et al., JINST, **3**, S08006 (2008).
[5] O. Adriani, et al., Phys. Lett. **B703**, 128 (2011).
[6] O. Adriani, et al., Phys. Lett. **B715**, 298 (2012).
[7] O. Adriani, et al., Phys. Rev. D, **86**, 092001 (2012).
[8] K. Werner, F. M. Liu and T. Pierog, Phys. Rev., **C74**, 044902 (2006).
[9] S. Ostapchenko, Phys. Rev., **D74**, 014026 (2006).
[10] E.-J. Ahn, R. Engel, T. K. Gaisser, P.Lipari and T.Stanev, Phys. Rev., **D80**, 094003 (2009).
[11] F. W. Bopp, J. Ranft R. Engel and S. Roesler, Phys. Rev., **C77**, 014904 (2008).
[12] T. Sjöostand, S. Mrenna and P. Skands, Comput. Phys. Comm., **178**, 852 (2008).
[13] T. Mase, et al., NIM, **A671**, 129 (2012).
[14] K. Kasahara, Proc. of 24th Int. Cosmic Ray. Conf. Rome 1, 399 (1995). EPICS web page, http://cosmos.n.kanagawa-u.ac.jp/
[15] L. Bonechi, et al., Proceedings of 29th ICRC, Pune,**vol.9**, 283 (2005).
[16] a la HMCMLL, see R. Barlow and C. Beeston, Comp. Phys. Comm. **77**, 219-228 (1993).